Molecular solvent model for an electrical double layer: Reference hypernetted-chain results for ion behavior at infinite dilution

G. M. Torrie
Department of Mathematics and Computer Science, Royal Military College, Kingston, Ontario K7K5L0, Canada

P. G. Kusalik[a] and G. N. Patey
Department of Chemistry, University of British Columbia, Vancouver, British Columbia, V6T1Y6, Canada

(Received 22 March 1988; accepted 25 May 1988)

We have extended our previous reference hypernetted-chain theory of the structure of a multipolar hard sphere fluid with water-like parameters in the vicinity of a large multiply charged macroion [J. Chem. Phys. 88, 7826 (1988)] to calculate the response of an isolated counterion to the charged surface of the macroion in this solvent environment. We have considered a range of macroion sizes from 28 to 84 Å and surface charge densities up to 17.5 $\mu C/cm^2$ (108 charges on a macroion 56 Å in diameter) and a range of counterion sizes from 1.9 to 4.0 Å. The ion–macroion potentials of mean force Φ_{im} in the solvent environment of the largest macroion are qualitatively different from those for more highly curved surfaces, in accordance with the previous predictions of the theory for the solvent reponse. Likewise, there is a relatively abrupt onset of oscillatory behavior in Φ_{im} at high surface charges, just as we found previously in the solvent structure under these conditions. At moderate surface charges, however, the ion response appears to assume an extraordinarily simple form in which Φ_{im} consists of two independent components, a short-range piece that is *independent of surface charge* and the simple Coulombic term that Φ_{im} approaches far from the surface. The mean electrostatic potential, on the other hand, has little resemblance to Φ_{im} and appears to be of limited usefulness in understanding the ionic distribution in a molecular solvent.

I. INTRODUCTION

In this paper we consider the question of how a molecular solvent mediates the interaction between an ion and a charged surface in an electrical double layer in the limit of infinite dilution.

Not surprisingly, statisical mechanical theories and models of interfacial phenomena such as this are frequently natural outgrowths of the previous development of analogous theories and models of the corresponding bulk systems. Certainly, this progression is evident in the treatment of continuum solvent models of the electrical double layer where the theoretical[1] and computer simulation[2] studies of the primitive model in the 1960's and 1970's led to similar advances by the same means a decade later for the corresponding model of the electrical double layer.[3–8] In this primitive model the solvent is characterized by only a single parameter, its dielectric constant, and has no molecular structure. However, despite the undisputed limitations of double layer models which fail to treat the solvent explicitly as a molecular species, the foundations for such an extension of double layer theory must lie in a prior understanding of similar molecular solvent models of bulk electrolyte solutions, and this has been slow to develop. For example, the establishment of a body of reliable simulation data for an electrolyte solution modeled at this level would require vast computational resources, even by current standards. No doubt, this perspective will change with time but one must be far less sanguine about the extraordinary convergence problems that are sure to plague such an enterprise if realistic potentials are to be used.[9] The additional boundary problems to be expected when a charged surface is introduced into such a polar fluid likely mean that the simulation of a full molecular solvent model of an electrified interface in a room temperature aqueous electrolyte is some time off as yet.

There have been some advances in analytic theories of electrolyte solutions, though, including the recent development of a general method for obtaining numerical solutions to the reference hypernetted-chain (RHNC) theory for molecular models.[10] The application of this general method to multipolar hard sphere models of electrolyte solutions[11] has provided a basis on which to construct similar theories of the double layer, a process we began in a recent paper[12] in which we considered only the solvent response to a charged surface for a hard sphere solvent with embedded dipole and quadrupole moments chosen to be similar to those in bulk liquid water. This was achieved by the simple expedient of solving the RHNC equations for a particular extreme case of a single ion immersed in this solvent: the "ion" was very large—its diameter was up to 30 times that of a solvent particle—and it carried a sufficient number of elementary charges—as many as 243—to exert a field in the adjacent solvent that was equivalent to that produced by surface charge densities typical of aqueous double layer systems. Despite the apparent isomorphism of such a system to the more familiar case of a small ion in solution, the solvent response to the macroion is quite different. In particular, for an *uncharged* macroion 30

[a] Present address: Research School of Chemistry, Australian National University, Canberra, Australian Capital Territory 2601, Australia.

 0021-9606/88/173285-10$02.10

times larger than a solvent molecule the RHNC theory predicts an ice-like solvent orientational structure in the surface layer that is very similar to that observed in computer simulation studies[13,14] of water models next to an uncharged planar surface. According to the RHNC theory for the multipolar hard sphere solvent, the tetrahedral coordination that characterizes the solvent orientations in this surface layer is largely preserved even in the presence of very high surface charges and no simple direct alignment of the molecular dipoles parallel to the surface field occurs, even in the contact layer. For moderate surface charge densities these unique structural features extend only a few angstroms from the surface after which only small deviations from the polarization density of a dielectric continuum are observed. This situation seems to change rather abruptly, however, around a surface charge density corresponding to 120 Å^2 per charge to one in which the solvent response (both the particle density and the polarization) develops marked oscillations that persist many solvent diameters out from the surface.

Here, we investigate the effect that this solvent response to the charged surface has on the potential of mean force between the surface and nearby isolated small ions by solving the RHNC equations for such systems. We begin in the following section by reviewing the details of the model and the RHNC equations for it. Our results for the potential of mean force are presented in Sec. III, where we discuss their dependence on the various parameters of the system and how they relate to both the previously determined solvent response and the continuum solvent picture. We conclude in Sec. IV with a summary and some observations on the relevance of the results to the structure of the double layer in systems at finite concentration.

II. MODEL AND RHNC THEORY

The system that we consider consists of three hard sphere species: solvent molecules of diameter $d_s = 2.8$ Å in which are embedded a point dipole μ and a point quadrupole of tetrahedral symmetry and magnitude Θ; a multiply charged macroion of diameter d_m; and a monovalent small ion of diameter d_i. The thermodynamic state of the solvent is determined by the dimensionless parameters $\rho_s^* = \rho_s d_s^3$, $\mu^* = \mu/\sqrt{d_s^3 kT}$ and $\Theta^* = \Theta/\sqrt{d_s^5 kT}$ which have the same numerical values here as in our previously reported work, viz., $\rho_s^* = 0.7317$, $\mu^* = 2.768$ and $\Theta^* = 0.968$. The relevance of these parameters to aqueous systems is discussed in Ref. 12.

The RHNC theory of this system comprises the Ornstein–Zernike equation

$$h_{\alpha\beta}(12) - c_{\alpha\beta}(12) = \frac{\rho_s}{8\pi^2}\int h_{\alpha s}(13)c_{\beta s}(23)d(3) \quad (1)$$

together with the closure relation

$$c_{\alpha\beta}(12) = h_{\alpha\beta}(12) - h_{\alpha\beta}^{\mathrm{HS}}(r) - \ln g_{\alpha\beta}(12) + \ln g_{\alpha\beta}^{\mathrm{HS}}(r) - u_{\alpha\beta}^{el}(12)/(kT) + c_{\alpha\beta}^{\mathrm{HS}}(r), \quad r \geqslant d_{\alpha\beta}, \quad (2)$$

$$h_{\alpha\beta}(12) = -1, \quad r < d_{\alpha\beta}.$$

In these equations the subscripts α and β take the values i, m, or s denoting ion, macroion, and solvent, respectively, and the superscript HS denotes a correlation function of the hard sphere reference mixture. $d_{\alpha\beta} = (d_\alpha + d_\beta)/2$ and $d(3) = d\Omega_3 d\mathbf{r}_3$ indicates integration over the position and orientational coordinates of particle 3. $h_{\alpha\beta}$, $c_{\alpha\beta}$, and $u_{\alpha\beta}^{el}$ denote, respectively, the total and direct pair correlation functions and the electrostatic part of the pair potential between species α and β; $g_{\alpha\beta} = h_{\alpha\beta} + 1$. The correlation functions of the hard sphere reference mixture required in this closure are obtained from a parameterization[15] of computer simulation results. The suitability of this procedure in the present context has been discussed elsewhere.[12]

The right-hand side of Eq. (1) would ordinarily contain a sum of convolutions over the three species in question but has only the solvent term in the present instance because both ionic species are present only at zero concentration. Consequently, the equations involving these species decouple and the solvent–solvent, ion–solvent, and macroion–solvent correlation functions are simply those that we have computed previously for the pure solvent,[16] the small ion in the pure solvent,[11] and the macroion in the solvent,[12] respectively. The only new quantity is the potential of mean force between the ion and the macroion, defined as

$$\Phi_{im}(12) \equiv -kT \ln g_{im}(12) \quad (3)$$

and using the RHNC closure, Eq. (2), this can be written as

$$\begin{aligned}\Phi_{im}(12)/kT &= -[h_{im}(12) - c_{im}(12)] + h_{im}^{\mathrm{HS}}(r) \\ &\quad - \ln g_{im}^{\mathrm{HS}}(r) - c_{im}^{\mathrm{HS}}(r) + u_{im}^{el}(r)/kT \\ &= -\frac{\rho_s}{8\pi^2}\int h_{is}(13)c_{ms}(23)d(3) \\ &\quad + h_{im}^{\mathrm{HS}}(12) - \ln g_{im}^{\mathrm{HS}}(r) \\ &\quad - c_{im}^{\mathrm{HS}}(r) + u_{im}^{el}(r)/kT. \end{aligned} \quad (4)$$

That is, Φ_{im} reduces to a simple convolution of h_{is} and c_{ms}; these are already available from our earlier work,[11,12] and therefore the calculation of Φ_{im} requires no iterative procedures and only trivial computational resources.

III. RESULTS AND DISCUSSION

The small ions and the macroion sizes and charges that we consider in what follows are perforce those of our previous work on those systems.[11,12] Thus, we discuss below results for macroions of diameter $10d_s$, $20d_s$, and $30d_s$ with negative surface charge densities σ of 0, -28, -56, and -108 where, as before, σ is the number of elementary charges that would be present on a macroion of diameter $20d_s$ (56 Å), regardless of the actual size of the macroion under discussion. The largest of these surface charge densities corresponds to about $-17.5\,\mu$C/cm^2 or 91 Å^2 per electron. The molecular symmetry of our solvent model is such that it interacts identically with a cation and an anion that have the same diameter and magnitude of charge; consequently, the ion–macroion potential of mean force depends only on the product of the signs of the ion and macroion charges rather than on each separately and it suffices to consider only one sign of the macroion charge. We have selected from among the small ion sizes used in the bulk solution work[11] those listed in Table I where they are labeled by the

TABLE I. Ion sizes in units of solvent diameters, $d_s = 2.80$ Å.

d_i/d_s	Counterion	Coion
0.68	Li^+	
0.84	Na^+	F^-
1.00	Eq^+	
1.16	Rb^+	Cl^-
1.28	Cs^+	
1.44	I^+	

names of the ions whose crystallographic radii motivated the choices of d_i. The ion labeled "Eq^+" in the Table has the same size as our solvent particles; the cation labeled "I^+" has the size used previously for the iodide ion but the opposite charge as we wish to consider it here as a counterion.

A. Relationship to the primitive model

Later in the discussion we shall consider the detailed dependence of Φ_{im} on the ion size and the macroion size and charge. However, in all cases Φ_{im} must, of course, approach the primitive model result,

$$\Phi_{im}(r) \sim Qq_i/(\epsilon r) \tag{5}$$

at large r, where Q and q_i are the macroionic and ionic charges, respectively, and ϵ is the dielectric constant of our solvent model ($\epsilon \doteq 93.5$).[11] Thus, it is natural to begin by asking what generalizations are possible concerning how quickly this asymptotic result is attained and how large might be the deviations from it close to the macroion surface. Here, and throughout our discussion of Φ_{im}, we shall find it helpful to consider its behavior within the context of the solvent response that we described previously.[12] For example, the solvent polarization density, or dipole moment per unit volume, $P(r)$ showed a relatively rapid attenuation to the continuum solvent result within three solvent diameters of contact so long as the surface charge density was not too large. This behavior changed relatively suddenly near $\sigma = -80$, however, to a pronounced oscillatory structure extending eight or more diameters from the surface.

There is a corresponding change in behavior for all the ion–macroion potentials of mean force that we have investigated. As an example, we show in Fig. 1 the results for Φ_{im} between the counterion Eq^+ and a $30d_s$ macroion over the full range of surface charge densities together with the continuum solvent asymptotes given by Eq. (5). For the neutral surface Φ_{im} is already sensibly zero at three solvent diameters from contact (the origin in Fig. 1) and the same may be said of the deviations of Φ_{im} from Eq. (5) for $\sigma = -28$ [Fig. 1(b)] and $\sigma = -56$ [Fig. 1(c)]. The *nature* of these deviations, namely the attractive well centered at about 0.6 d_s from contact, turns out *not* to be a universal feature but the various deviations of Φ_{im} from the primitive model asymptote that we discuss below for different counterions share this common characteristic of rapid attenuation within $3d_s$ of contact. The behavior of Φ_{im} at $\sigma = -108$, however, is altogether different, with regularly spaced, gradually damped oscillations about the continuum result extending far into the solvent. For the particular case of the Eq^+ ion

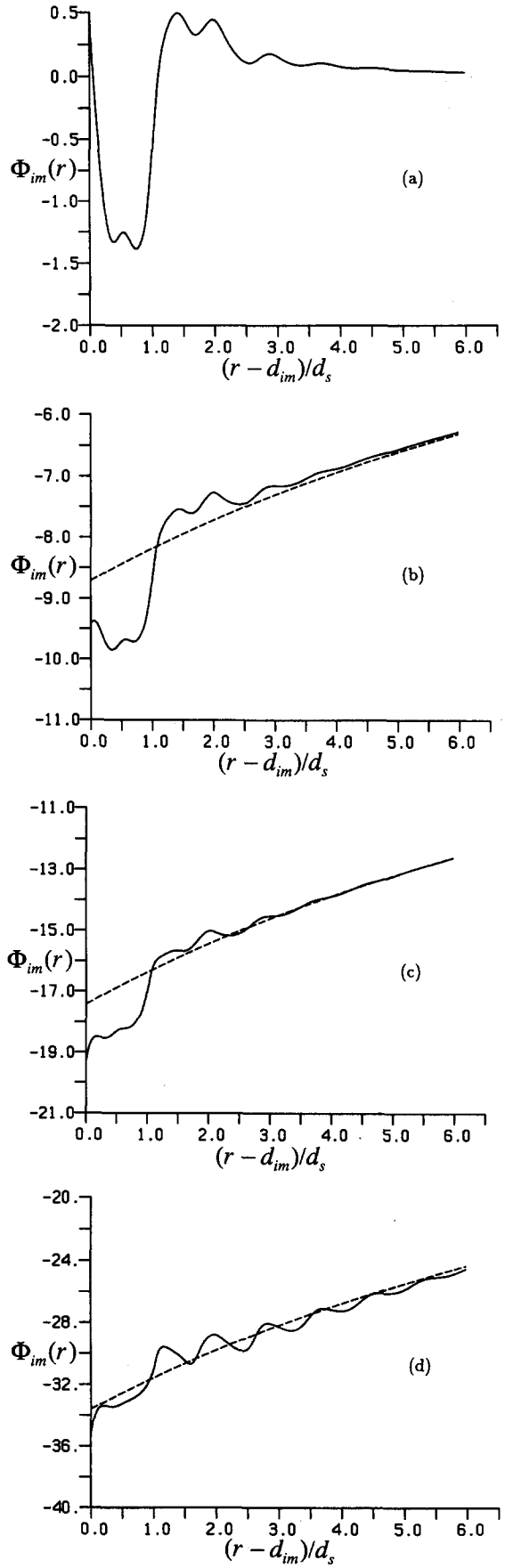

FIG. 1. Potential of mean force Φ_{im} between a $30d_s$ macroion and a counterion Eq^+ of diameter d_s for various surface charge densities σ; (a) $\sigma = 0$; (b) $\sigma = -28$; (c) $\sigma = -56$; (d) $\sigma = -108$. (—)RHNC theory for molecular solvent; (- - -) result for a dielectric continuum. (Note: in all figures the vertical axis is marked in units of kT.)

shown in Fig. 1 these oscillations happen to be exactly in phase with the corresponding oscillations in the solvent response that we reported earlier,[12] the minima in Φ_{im} coinciding with the maxima in the magnitude of the solvent polarization and density profiles. The situation is more complex for ions of different size whose behavior we describe below, but it remains true that Φ_{im} for all ions that we considered exhibits this qualitative change to oscillatory behavior for large σ driven by the similar change predicted previously by the theory for the solvent response.

The scales necessary to show Φ_{im} in Fig. 1 (the vertical scale factor doubles in successive panels) give the impression that the deviations of Φ_{im} from the simple primitive model picture are small for all surface charges. This is true in a sense, but because these differences occur on a molecular distance scale the mean *forces* which they imply are very different from the continuum theory predictions, not only in magnitude but often in direction as well. There are also corrections to the simple Coulombic potential of mean force that are less intimately related to the details of the local solvent structure and which arise from more general considerations of polarization effects.[17] Our numerical evidence suggests, however, that for $|\sigma| < 80$ where such effects would not be obscured by the oscillatory response typical of larger surface charges, these corrections must be quite small despite the larger charges and diameters that characterize the macroionic species of the present model. For example, the deviations of Φ_{im} from the Coulombic asymptote in Figs. 1(b) and 1(c) beyond the region near contact are very small, have no apparent systematic dependence on ion size or macroion charge and, in any case, are probably not significant with respect to the precision of our numerical procedures. (When a small uncharged solute is substituted for the ion then Φ_{im} does exhibit a clearly discernible long-range tail. This is discussed in Sec. III D and in the Appendix.)

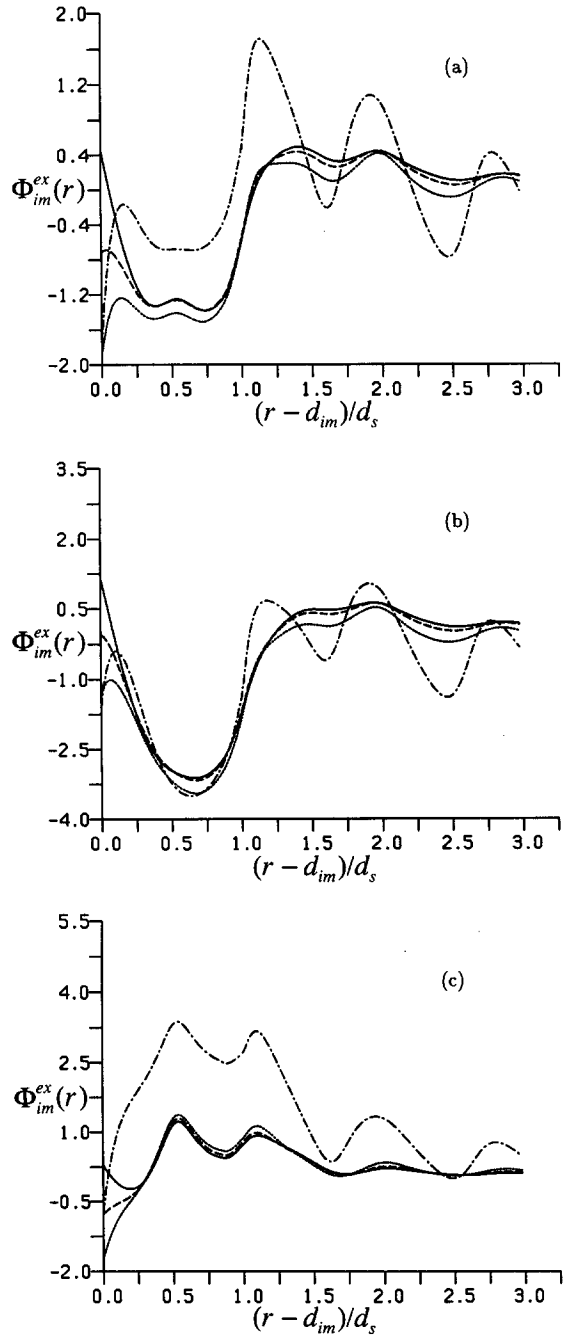

FIG. 2. Excess potential of mean force Φ_{im}^{ex} between a $30d_s$ macroion and the counterions (a) Eq^+; (b) Na^+; (c) Cs^+ for various surface charge densities σ. (—)$\sigma = 0$; (- - -)$\sigma = -28$; (···)$\sigma = -56$; (-·-·-·)$\sigma = -108$.

B. Dependence on surface charge

The data in Fig. 1 suggest strongly that for all but the highest surface charge density the *excess* potential of mean force defined as

$$\Phi_{im}^{ex} \equiv \Phi_{im} - Qq_i/(\epsilon r) \tag{6}$$

is relatively insensitive to the magnitude of the surface charge [and hence remains similar to $\Phi_{im}(\sigma = 0)$]. This is also a reasonable expectation in light of the earlier predictions of the theory for the solvent response to the surface charge.[12] All the same, these qualitative considerations fall far short of anticipating the appearance of the data of Fig. 1 when replotted in terms of Φ_{im}^{ex} as we have done in Fig. 2(a). Except for a small region within $0.2d_s$ of contact, the three curves in this Figure representing Φ_{im}^{ex} for $\sigma = 0$, -28, and -56 are practically congruent, implying that the nontrivial component of the response of the ion to the charged surface is virtually independent of the density of that charge up to 176 Å^2 per electron, i.e., for most of the range relevant to physical systems. For the $30d_s$ macroion, the flattest surface that we have studied, the response of all ions exhibits this same indifference to the surface charge even though the shape of Φ_{im}^{ex} itself is very sensitive to ion size. For example, Φ_{im}^{ex} for the smaller Na^+ ion, shown in Fig. 2(b), has a much deeper attractive well than the Eq^+ case of Fig. 2(a) but only slightly more variation with surface charge for $|\sigma| \leqslant 56$, perhaps because this smaller ion couples more strongly to the solvent and so is more sensitive to small changes in the local solvent structure. Φ_{im}^{ex} for the Cs^+ ion [Fig. 2(c)], on the other hand, has a repulsive peak near $0.5d_s$ from contact in place of the attractive well characterizing the smaller ions, yet this structure shows even less change with surface charge for $|\sigma| \leqslant 56$.

When we originally applied the RHNC theory to the

solvent structure our analysis of the macroion–solvent angular correlation functions in the case of an uncharged $30d_s$ macroion seemed to confirm the earlier discovery in computer simulations of a dominant ice-like structure near the surface, characterized by tetrahedral coordination with one hydrogen bond of each molecule in the contact layer being directed into the surface. For a moderately charged surface, analysis of these same correlation functions suggested that this structure was essentially unaltered by the electric field, in the sense that the molecular dipoles tend to maintain the oblique angle to the surface normal required by the tetrahedral coordination of the zero-field structure rather than rotating into parallel alignment with the field. The polarization of the solvent in this region appears to arise from a preference for those oblique dipole orientations whose *component* along the field direction is energetically favorable. In terms of this picture, then, the short-range structural features of Φ_{im}^{ex}, being independent of σ, presumably arise from that ion's response to this local ice-like solvent arrangement; the effect of a surface charge is simply to superimpose on this the trivial continuum asymptote *at all distances*. An amusing corollary of this lack of dependence of Φ_{im}^{ex} on the surface charge concerns the relationship of Φ_{im}^{ex} for a negatively charged coion to Φ_{im}^{ex} for the counterion of the same size. For the *uncharged* surface these two Φ_{im}^{ex} are identical by definition in our model owing to the symmetry of the molecular quadrupole tensor of the solvent. Even for a charged surface, however, the solvent response is such that the counterion and coion Φ_{im}^{ex} are practically coincident; this is illustrated in Fig. 3 on which we have plotted the excess potential of mean force for two such counterion–coion pairs, Na^+, F^- ($d_i = 0.84d_s$), and Rb^+,Cl^- ($d_i = 1.16d_s$) with a $30d_s$ macroion at $\sigma = -28$. Despite the noticeable size dependence of Φ_{im}^{ex} in this figure, a point to which we return below, the difference between the curves for a counterion and a coion of equal size is scarcely discernible, except for an easily understood divergence in the small region very close to contact.

At high surface charge densities the situation is entirely different. Φ_{im}^{ex} becomes a long-range oscillatory function in concert with the similar changes in the solvent behavior that we have already mentioned. The excess quantities in Fig. 2 serve to emphasize even further this dramatic change in the response of the system; this is especially true of Φ_{im}^{ex} for larger ions such as Cs^+ where there is almost no dependence on surface charge until this qualitative change takes place.

Despite the similarity in size of the counterions Na^+ and Rb^+, their Φ_{im}^{ex} in Fig. 3 are not much alike. This sensitivity to counterion size—the only variable parameter in our solution model—is a general feature of our results and in Fig. 4(a) we illustrate this for the full range of counterion sizes for the case of an uncharged $30d_s$ macroion. (Of course, these Φ_{im} at $\sigma = 0$ are representative of Φ_{im}^{ex} for all $|\sigma| \leqslant 56$.) For counterions that are smaller than the solvent the principal feature of Φ_{im} is an attractive well centered near $0.6d_s$ from contact, i.e., immediately adjacent to the peak of more than $3\rho_s$ in the solvent density lying closer to the surface.[12] This well is especially deep for the $0.68d_s$ ion we call Li^+; although this is a plausible prediction of the theory for the response of such a small hard sphere ion to the high solvent density, the model itself is unlikely to be very appropriate for representing the behavior of strongly hydrated lithium ions in solution. As the counterion size increases this attractive well is gradually supplanted by a repulsive peak whose height grows until it exceeds $3kT$ for the counterion I^+. As it

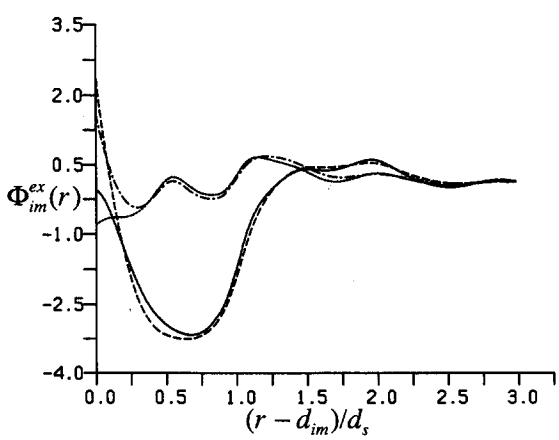

FIG. 3. Φ_{im}^{ex} between a $30d_s$ macroion with $\sigma = -28$ and equal-sized counterions and coions. (—)Na^+, $d_i = 0.84d_s$; (- - -)F^-, $d_i = 0.84d_s$; (···)Rb^+, $d_i = 1.16d_s$; (-·-·-·)Cl^-, $d_i = 1.16d_s$.

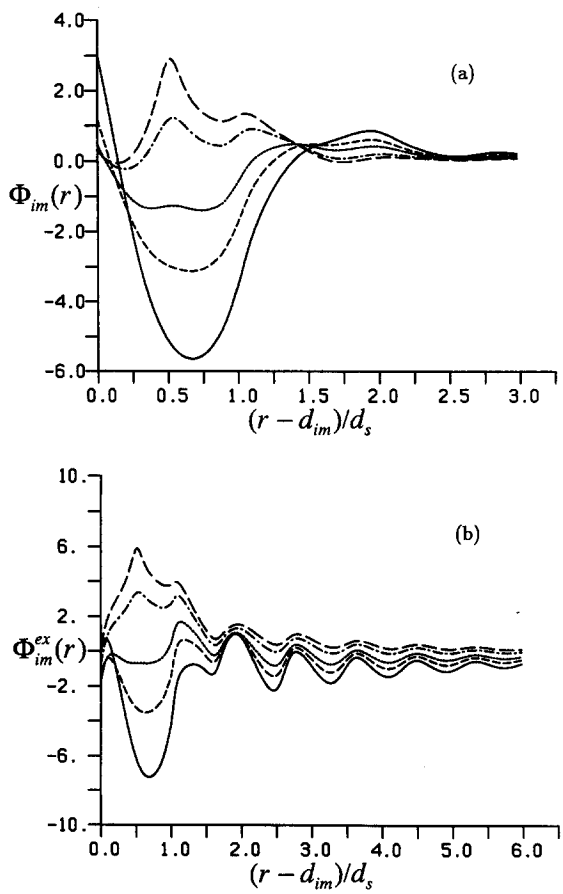

FIG. 4. (a) Potential of mean force Φ_{im} between an uncharged $30d_s$ macroion and various counterions; (—) Li^+; (- - -) Na^+; (···) Eq^+; (-·-·-·) Cs^+; (— — —) I^+. (b) Excess potential of mean force Φ_{im}^{ex} between a $30d_s$ macroion and various counterions at $\sigma = -108$, symbols as in (a).

happens, there is a similar peak at just this location in the potential of mean force of the underlying hard sphere reference system (but for *all* ions of course, not just the larger ones). However, the behavior shown in Fig. 4(a) must be regarded as a solvation phenomenon rather than as an excluded volume effect, not only on the basis of the contrary behavior of the smaller ions, but because the solvent density has a local minimum near this point in any case.

In Fig. 4(b) we show the dependence of Φ_{im}^{ex} on counterion size for the highly charged $30d_s$ macroion, $\sigma = -108$. The spectrum of behavior near contact has been spread relative to the $\sigma = 0$ case of Fig. 4(a); this subtle effect may be a manifestation of both excluded volume and solvation effects arising from a secondary solvent density peak that develops near $0.6d_s$ at high surface charge [cf. Fig. 4(b) of Ref. 12]. Perhaps as well, the increased rigidity of the solvent structure in this high field enhances its discrimination of the solubility differences among the larger counterions. At larger distances all Φ_{im}^{ex} exhibit similar oscillatory behavior, apparently in response to the corresponding behavior of the solvent to high surface charge density. Notice, however, that the nearly precise registry of these oscillations for different sized ions in this figure is a consequence of our use of an ion-dependent origin, namely, the distance of closest approach of an ion to the surface. In fact, only for the Eq^+ ion is Φ_{im}^{ex} exactly in phase with the solvent behavior in the manner that we described in the discussion of Fig. 1 in Sec. III A; the phase shift from this of Φ_{im}^{ex} for any other ion must equal that ion's hard sphere radius in order to account for the coherence evident in Fig. 4(b) where the potentials for a variety of ions have been plotted in terms of this reduced distance. This is one of the few similarities of Φ_{im} to the RHNC predictions for the potentials of mean force between pairs of small ions in the bulk solution.[11]

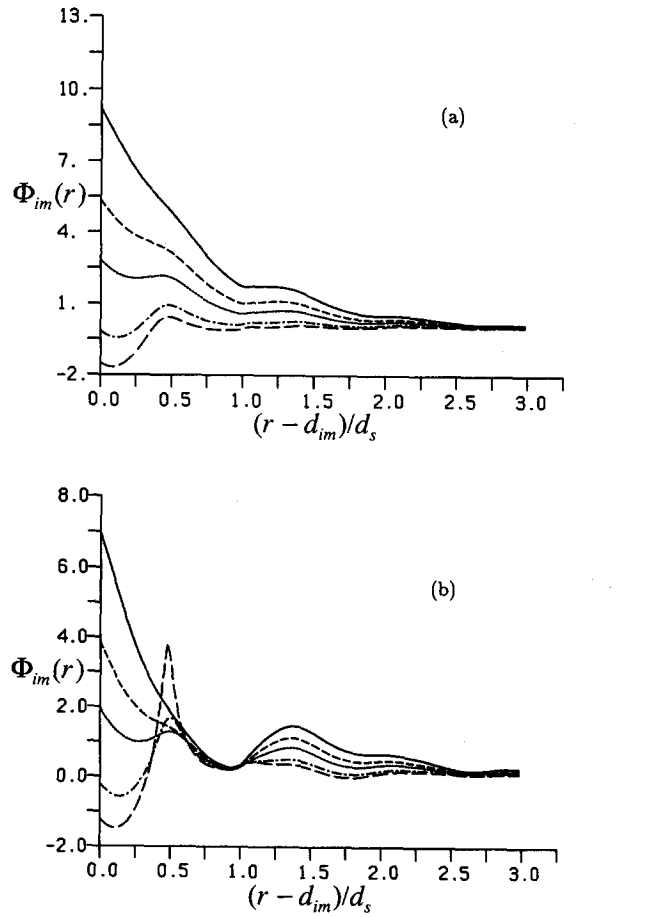

FIG. 5. Potential of mean force between smaller uncharged macroions and various counterions (a) $d_m = 10d_s$; (b) $d_m = 20d_s$. Symbols as in Fig. 4(a).

C. Dependence on surface curvature

If it is the details of the local solvent structure that determine the excess ion–macroion potential of mean force then we must expect Φ_{im}^{ex} for $10d_s$ and $20d_s$ macroions to be quite different from those for the flatter $30d_s$ systems we have been describing thus far. This is because the distinctive angular distributions that are the signature of the solvent structure next to a $30d_s$ macroion—and which computer simulations confirm, at least for $\sigma = 0$—do not develop gradually as d_m increases. Instead, these angular distributions for $10d_s$ and $20d_s$ macroions are rather similar to each other and, roughly speaking, seem to represent an intermediate case between the solvent arrangement around small ions and the planar-like stucture evident when $d_m = 30d_s$; the peak in the solvent density near these smaller macroions is also much lower than for the flatter macroion.

We have plotted the potentials of mean force Φ_{im} for uncharged macroions of diameter $10d_s$ in Fig. 5(a) and $20d_s$ in Fig. 5(b) for the same set of counterion sizes used in Fig. 4(a) for the $30d_s$ case to which they should be compared. The dominant feature of this comparison is the complete inversion of the trend with respect to ion size of the shape of these curves near $0.5d_s$ from contact in passing from the $10d_s$ macroion to the $30d_s$ systems. In the former case Φ_{im} is purely repulsive for the smaller ions with a very shallow attractive well at contact gradually developing to a depth of $2kT$ for the iodide ion. For the $30d_s$ macroion, on the other hand, Φ_{im} for these same smaller ions is characterized instead by an attractive well near $0.5d_s$ from contact which gives way with increasing ion size to a repulsive peak in the same location. It is really the small ions that are driving this turnabout in behavior: contrast the relatively small shifts in Φ_{im} for the larger ions between Figs. 5(a) and 4(a) with the complete reversal characterizing the potentials for Na^+ in the same two figures. This is consistent with a conjecture that we made in Sec. III B while considering the charge dependence of Φ_{im}^{ex} for various ions, that the smaller ions are more sensitive probes of changes in the solvent structure near the surface.

The potentials for the $20d_s$ case in Fig. 5(b), while intermediate between those in Figs. 5(a) and 4(a), clearly resemble more closely those for the smaller macroion, as our review of the solvent behavior had anticipated. A notable exception is the repulsive peak in Φ_{im} for the iodide ion at $0.5d_s$ from contact which is narrower and higher here than for either the $10d_s$ or $30d_s$ cases. The principal contribution to this anomaly turns out to come from the potential of mean force of the underlying hard sphere reference system. The algorithm that we use for this is based on corrections to the

Percus–Yevick theory of hard sphere mixtures and breaks down when applied to the case of two large spheres at infinite dilution in a bath of much smaller ones. That this shortcoming of the theory has manifested itself here rather than for the same large ion (for I^+, $d_i = 1.44d_s$) and a $30d_s$ macroion suggests that similarity in size of the two large impurities may exacerbate the effect. In any case, we regard the peculiar behavior of Φ_{im} for this ion in Fig. 5(b) as far more likely to have arisen from deficiencies in our approximation for the reference system than from a real physical effect.

We have not shown the behavior of Φ_{im}^{ex} when these smaller macroions are charged since it is entirely predictable from the observations we have already made for the $30d_s$ systems of Figs. 2 and 4. That is, although the solvent structure and, with it, the Φ_{im}^{ex} are different for these smaller macroions in the ways we have just described, it remains true that for charged surfaces up to $\sigma = -56$ they are very similar to the Φ_{im} ($\sigma = 0$) in Fig. 5, and that the onset of oscillatory behavior in the solvent for $|\sigma| \geqslant 80$ which occurs as well for these smaller macroions is likewise tracked by similar behavior in Φ_{im}^{ex}. More generally, one would like to be able to offer a more satisfying rationale for the great sensitivity of Φ_{im} to the changes in the solvent structure that arise when $d_m > 20d_s$. Unfortunately, the correlation functions that would be most helpful in this regard are those that describe the ion–solvent structure in the presence of the macroionic surface, and these are three-body functions not given by the homogeneous RHNC theory that we have applied.

D. Neutral solutes

Between two small neutral particles in our solvent there would be a potential of mean force with a deep attractive well at contact as the highly structured polar solvent seeks to expel such hydrophobic solutes. This should not change if one of the two solutes in question is charged and, furthermore, in such a case the neutral solute would not be expected to be very sensitive to local changes in the solvent structure induced by the ion. These considerations can be extended unmodified to account for the potential of mean force between small uncharged solutes and the *smaller* macroions of diameter $10d_s$ and $20d_s$. The solid and dashed lines in Fig. 6 illustrate this for an uncharged solute equal in size to the solvent next to these two macroions, each carrying our largest suface charge, $\sigma = -108$. The attractive wells at contact in both these cases are very similar to those that we calculated for the same systems without any charge on the macroions and to those for neutral solutes of different sizes; in addition, the potentials of mean force in this figure have clearly not responded to the oscillatory behavior of the solvent at this high surface charge. All this is in accordance with the expectations expressed above. For our largest macroion these same observations regarding the indifference of Φ_{im} to solute size and high macroion charge with its attendant oscillatory polarization still apply, but the hydrophobic well at contact is now shielded from the bulk solution by a repulsive peak near $0.5d_s$ (dotted line in Fig. 6). Presumably, this has developed because the high density and degree of orientational order in the solvent that characterize the flatter surface form an especially inhospitable environment

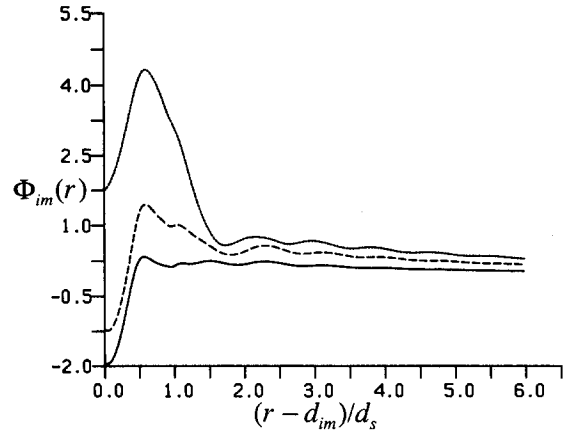

FIG. 6. Potential of mean force between different sized macroions and a neutral solute of diameter $d_i = d_s$ at $\sigma = -108$; (—)$d_m = 10d_s$; (- - -) $d_m = 20d_s$; (···)$d_m = 30d_s$.

for the neutral solute. The height of this peak is sufficient to pose a kinetic barrier of some consequence to the coagulation expected from the hydrophobic effect, but this observation must be tempered by one that we made previously[12] concerning the likely dependence of the solvent density peak on the hard sphere forces of our model; more realistic potentials show much smaller density maxima.[13,14]

One additional feature of the potentials in Fig. 6 that deserves comment is their evident slow repulsive decay at large separations. This tail, which extends far beyond the distances shown in the figure, is entirely absent when the macroion is uncharged, yet has virtually no oscillatory character which suggests that its physical origin must be related to the long-range polarization of the solvent. This intuitive notion can be rendered more precise through a consideration of the asymptotic behavior of the macroion–solvent direct correlation function as described in the Appendix. The argument given there shows that the tail in Φ_{im} has a complex functional form that is a consequence of competition between attractive as well as repulsive solvent effects. In an electrically neutral system, of course, the solvent polarization will be short ranged due to screening and this repulsive tail will not be present.

E. Mean electrostatic potential

The customary way of making contact, albeit indirectly, between theories of the microscopic structure of electrified interfaces and experimental data on real systems has been through the differential capacitance which depends in turn on the drop in electrostatic potential Ψ between the surface and the bulk solution. Although the systems described in this paper are not true double layers—there is only a single counterion responding to the charged surface of the macroion and the electrostatic screening characteristic of a system with overall electrical neutrality is absent—they still serve to illustrate quite dramatically a final point we wish to make concerning the difficulty of using an essentially macroscopic quantity such as Ψ in a molecular solvent model.

There is no difficulty in *defining* $\Psi(r)$, the mean electrostatic potential at a distance r from the center of the ma-

croion. In fact, for the systems under consideration here the zero-concentration counterion cannot affect $\Psi(r)$ which continues to depend on the Coulombic field of the macroionic charge Q and the solvent response to that field in the way expressed by Eq. (6) of Ref. 12. Far from the surface both $\Psi(r)$ and $\Phi_{im}(r)/q_i$ approach the common Coulombic asymptote of $Q/(\epsilon r)$ but the counterion-independent $\Psi(r)$ obviously cannot account for the variety of behavior in Φ_{im} close to the surface that we have encountered. More importantly, though, close to the surface $\Psi(r)$ differs from this asymptote by several orders of magnitude and has a very high *repulsive* peak at the contact distance of a solvent molecule with the surface, just where we might expect to have the highest probability of finding a counterion.[12] By comparison, the counterion potentials of mean force that we have reported here exhibit important but much more modest deviations from the continuum result, a difference which we have illustrated in Fig. 7 by superimposing the excess mean electrostatic potential $\Psi^{ex}(r) \equiv \Psi(r) - Q/(\epsilon r)$ and $\Phi^{ex}_{im}(r)$ for the $30d_s$–Eq^+ system at moderate charge [$\sigma = -28$, Fig. 7(a)] and at high charge [$\sigma = -108$, Fig. 7(b)]. The disparity in magnitude of these two excess quantities has necessitated the use of a vertical scale compression of five in these figures for Ψ^{ex}; even this is altogether insufficient to contain the contact peak of nearly 90 kT in this quantity for $\sigma = -108$. Within the context of the homogeneous Ornstein-Zernike equations which we have used here to describe

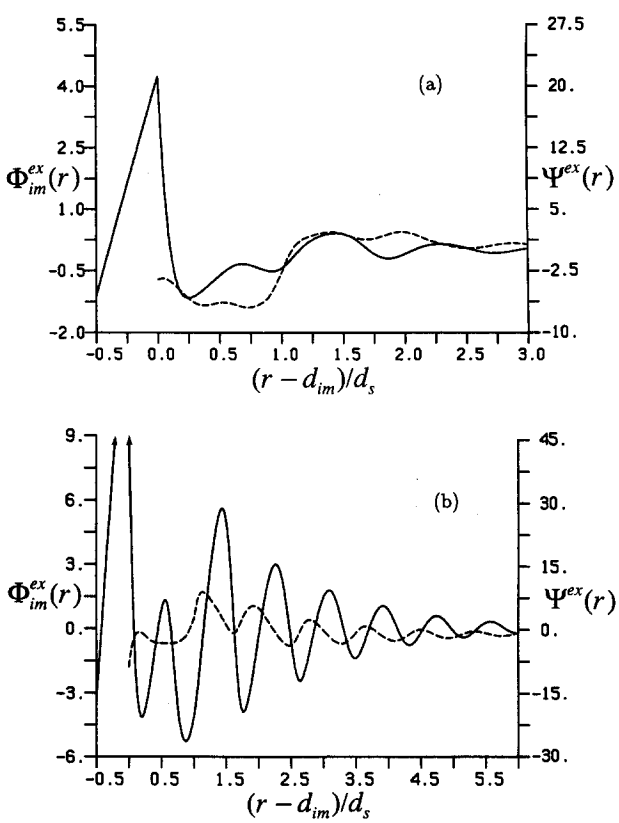

FIG. 7. Excess electrostatic potential Ψ^{ex} and excess potential of mean force Φ^{ex}_{im} between a $30d_s$ macroion and the counterion Eq^+ (a) $\sigma = -28$; (b) $\sigma = -108$. (—) Ψ^{ex}; (- - -) Φ^{ex}_{im}. Note the right-hand scale for Ψ^{ex} is compressed by a factor of 5.

the macroion–solvent interface, Ψ and Φ_{im} would coincide for a zero-concentration counterion that had *only* Coulombic interactions with the solvent. In this sense, the difference between these two quantities is ultimately attributable to the short-range forces in the intermolecular potential, hard sphere forces in the present instance. Inevitably, this makes the relationship between these two quantities complex and difficult to interpret in the absence of the sort of information that would be forthcoming from computer simulation or even a truly inhomogeneous theory. For example, Φ^{ex}_{im} for both surface charges in Fig. 7 has a broad attractive well near $0.6d_s$ whereas Ψ^{ex} has a local maximum near here in each case. For the highly charged surface both Φ^{ex}_{im} and Ψ^{ex} oscillate with about the same period, but not in phase. As we pointed out in the earlier discussion of Fig. 4(b), Φ^{ex}_{im} for the ion Eq^+ happens to oscillate in phase with the solvent density and polarization profiles (and so Ψ^{ex} evidently does not) but for other ions even this coherence of Φ^{ex}_{im} with the solvent response is disrupted by hard sphere effects. What *is* clear from Fig. 7, however, is that the distribution of counterions near the surface has no relationship whatsoever to the high degree of variation in $\Psi(r)$, particularly the large repulsive peak at the solvent contact distance.

IV. CONCLUSION

The unique properties of the solvent structure next to the macroion surface that emerged from our previous calculations[12] provide a natural framework for interpreting the present predictions of the RHNC theory for the response of small ions to this solvent environment as expressed by the ion–macroion potential of mean force. For example, the distinctive solvent orientational arrangement found in computer simulations for a planar surface was clearly established in the RHNC theory of our model only for the largest macroion, $d_m = 30d_s$. Although there was evidence that this structure was beginning to develop for more highly curved surfaces, the results for $10d_s$ and $20d_s$ macroions were more similar to each other than to those for the $30d_s$ case. This is reflected in the ion–macroion potentials of mean force perhaps more vividly than in the solvent properties themselves through the inversion of the order of Φ^{ex}_{im} for various counterions that occurs between Figs. 4(a) and 5. This inversion comes about primarily because of the sensitivity of Φ^{ex}_{im} to the hard sphere diameter of the ions, especially once $d_i \leqslant d_s$, and is not unexpected in view of the similar variety of behavior found in the potentials of mean force between pairs of small ions in bulk solution.[11] The details of these variations for the present hard sphere models are perhaps primarily of theoretical interest, but their very existence demonstrates a more fundamental reality to be confronted here as well as in the theory of bulk electrolyte solutions namely, that the variety of behavior in real systems guarantees that the properties of realistic molecular models will likewise exhibit strong dependence on the details of the intermolecular potentials. For an interfacial problem such as the double layer a theory based, like the present one, on the homogeneous Ornstein–Zernike equation is of limited value in elucidating these questions of detail in any case. Ultimately, information

about the counterion response to the inhomogeneous solvent environment near the surface will be needed, and this will have to come from computer simulation and theories expressly designed for inhomogeneous systems.[18]

The most interesting aspects of the solvent behavior, though, were the ways in which its structure responded to the charge on the macroion, and this is true of the ion–macroion potentials of mean force as well. For both the solvent and the counterion response there is a qualitative change in behavior that occurs around $\sigma = -80$. For smaller charges the solvent polarization occurs without significant disruption of the intermolecular correlations established in response to the presence of the uncharged surface; the corresponding invariant of the ion response turns out to be the excess potential of mean force relative to the Coulombic asymptote as defined in Eq. (6). That is, to an excellent approximation, *the charge-dependent part of the ion–macroion potential of mean force at all distances is simply Coulomb's law* (with the dielectric constant of the bulk solvent). The full potential of mean force is obtained by decorating this with the addition of $\Phi_{im}(\sigma = 0)$. The symmetric solvation properties of our solvent model with its tetrahedral quadrupole may be partly responsible for this remarkable result, but we suspect that the most important characteristic of the solvent model in this regard is the resistance of its strong intermolecular couplings to the perturbing field of the charged surface. We have argued before[12] that this is likely to be a general property of more realistic water models near charged surfaces in which case the simple decomposition of the ion–surface potential of mean force that we have found in the present model could serve as a very useful conceptual paradigm for the double layer problem in general. Certainly, something will be needed to replace the notion, so useful for the continuum solvent primitive model double layer, of an ionic distribution determined largely by a self-consistent mean electrostatic potential, gently perturbed by ion–ion correlations.

There are two fundamental differences between the solvent response to a macroion and the solvent restructuring around a small solute that preclude a similar simple decomposition of the potential of mean force between small ions. To begin with, the solvent structure around a small uncharged solute lacks the specific orientational order and associated rigidity that seems to characterize the response of a water-like solvent to a smooth planar surface. Second, a fully charged small ion exerts a much stronger electric field than any realistic surface charge on our macroion would and so has a much greater effect on the solvent structure. The same sort of thing begins to happen for the macroion system only for $|\sigma| \geqslant 80$ and is signaled by the onset of oscillations in the solvent density and polarization profiles. When this happens, similar oscilltions develop in the ion response and the charge independence of Φ_{im}^{ex} is destroyed.

The present results for single counterions suggest some intriguing possibilities for the theoretical description of the double layer that will form about the macroion in a finite concentration electrolyte. At least for low concentrations, it is plausible that the resulting finite counterion atmosphere near the surface will not affect the principal qualitative features of the solvent response at infinite dilution and that the solvent structure will continue to be insensitive to surface charge in the sense that we have described. In that event, the counterion potential of mean force might well continue to be separable, as we found it to be here, into a short-range component representing the ion response to the local solvent structure, and a long-range term arising from the ionic forces in the system. This latter term was simply Coulomb's law for the infinite dilution system we considered here, but would itself become a nontrivial function of the electrolyte concentration in the many-ion system, although it might turn out to be similar to the corresponding function in the primitive model double layer. At higher surface charges the situation seems certain to be more complicated since the oscillations characterizing the response at infinite dilution extend to distances comparable with the screening lengths of the finite concentration systems. We are presently investigating these questions through the RHNC theory for macroions in electrolytes over a range of concentrations.

ACKNOWLEDGMENTS

This work was begun while G.M.T. was visiting the University of British Columbia on sabbatical leave and he is happy to acknowledge the hospitality extended to him by the Department of Chemistry there. This work has been supported in part by the Defence Research Board of Canada under ARP Award No. 3610-645, and in part by the Natural Sciences and Engineering Research Council of Canada.

APPENDIX: THE POTENTIAL OF MEAN FORCE BETWEEN A CHARGED MACROION AND A NEUTRAL HARD SPHERE AT LARGE SEPARATIONS

From Eq. (4) it follows that as $r_{nm} \to \infty$,

$$\Phi_{nm}(12)/kT \sim -\frac{\rho_s}{8\pi^2}\int h_{ns}(13)c_{ms}(23)d(3), \quad \text{(A1)}$$

where the subscripts n, m, and s designate the neutral hard sphere, macroion, and solvent particle, respectively. Also it is obvious that since $h_{ns}(13)$ is short ranged only the long-range asymptotic behavior of $c_{ms}(23)$ will contribute to the convolution in the limit $r_{nm} \to \infty$. This means that when $c_{ms}(23)$ is expanded in rotational invariants [cf. Eqs. (4a), (5), and (36) of Ref. 10] the only projections which need be considered are $c^{000}_{00;ms}(r_{ms})$ and $c^{022}_{00;ms}(r_{ms})$. As $r_{ms} \to \infty$ it can be shown[12] that these take the form

$$c^{000}_{00;ms}(r_{ms}) \sim \frac{1}{6}\frac{A^2}{r_{ms}^4} + O\left(\frac{1}{r_{ms}^8}\right) + \cdots, \quad \text{(A2a)}$$

$$c^{022}_{00;ms}(r_{ms}) \sim \frac{1}{3}\frac{A^2}{r_{ms}^4} + O\left(\frac{1}{r_{ms}^8}\right) + \cdots, \quad \text{(A2b)}$$

where $A = 3Q(\epsilon - 1)/(4\pi\rho_s\mu\epsilon)$. For an ion in the dipole tetrahedral–quadrupole solvent there are additional projections in the expansion of $h_{is}(12)$ that will also contribute to slow algebraic decay in c_{ms} but which do not need to be considered for the present case of a neutral solute.

Substituting Eqs. (A2) into Eq. (A1) and using the orthogonality properties of the rotational invariants immediately yields

$$\Phi_{nm}(r_{nm})/kT \sim -\frac{A^2}{6}\rho_s \int h^{000}_{00;ns}(r_{ns})\left(\frac{1}{r^4_{ms}}\right) d\mathbf{r}_{ns} - \frac{4A^2}{15}\rho_s \int h^{022}_{00;ns}(r_{ns})\left(\frac{1}{r^4_{ms}}\right) d\mathbf{r}_{ns}, \quad \text{(A3)}$$

where for convenience we have placed the neutral sphere at the origin. Then using spherical polar coordinates such that $d\mathbf{r}_{ns} = \sin\theta d\theta\, d\phi\, r^2_{ns}\, dr_{ns}$ and carrying out the integrations on θ and ϕ we obtain

$$\Phi_{nm}(r_{nm})/kT \sim -\frac{2\pi}{3}A^2\rho_s \int \frac{r^2_{ns}}{(r^2_{nm}-r^2_{ns})^2} h^{000}_{00;ns}(r_{ns})dr_{ns} - \frac{16\pi}{15}A^2\rho_s \int \frac{r^2_{ns}}{(r^2_{nm}-r^2_{ns})^2} h^{022}_{00;ns}(r_{ns})dr_{ns}. \quad \text{(A4)}$$

For hard core models $h^{000}_{00;ns}(r_{ns}) = -1$ and $h^{022}_{00;ns}(r_{ns}) = 0$ if $r_{ns} < d_{ns}$, and the integrals occurring in Eq. (A4) can be partially performed analytically to give

$$\Phi_{nm}(r_{nm})/kT \sim \frac{2\pi}{3}A^2\rho_s\left[\frac{d_{ns}}{2(r^2_{nm}-d^2_{ns})} - \frac{1}{4r_{nm}}\ln\left(\frac{r_{nm}+d_{ns}}{r_{nm}-d_{ns}}\right)\right] - \frac{2\pi}{3}A^2\rho_s\int_{d_{ns}}^{\infty} \frac{r^2_{ns}}{(r^2_{nm}-r^2_{ns})^2} h^{000}_{00;ns}(r_{ns})dr_{ns} - \frac{16\pi}{15}A^2\rho_s \int_{d_{ns}}^{\infty} \frac{r^2_{ns}}{(r^2_{nm}-r^2_{ns})^2} h^{022}_{00;ns}(r_{ns})dr_{ns}. \quad \text{(A5)}$$

Since in Eqs. (A2) we have included only terms which decay more slowly than r^{-8}_{ns} we can expect Eq. (A5) to be exact only to order r^{-6}_{nm}. Therefore, expanding Eq. (A5) we obtain the final result

$$\Phi_{nm}(r_{nm})/kT \sim \frac{2\pi}{3}A^2\rho_s\left(\frac{1}{3}\frac{d^3_{ns}}{r^4_{nm}} + \frac{2}{5}\frac{d^5_{ns}}{r^6_{nm}} + \cdots\right) - \frac{2\pi}{3}A^2\rho_s\int_{d_{ns}}^{\infty}\left(\frac{r^2_{ns}}{r^4_{nm}} + \frac{2r^4_{ns}}{r^6_{nm}} + \cdots\right)h^{000}_{00;ns}(r_{ns})dr_{ns} - \frac{16\pi}{15}A^2\rho_s\int_{d_{ns}}^{\infty}\left(\frac{r^2_{ns}}{r^4_{nm}} + \frac{2r^4_{ns}}{r^6_{nm}} + \cdots\right)h^{022}_{00;ns}(r_{ns})dr_{ns}, \quad \text{(A6)}$$

which for the present model gives the correct limiting behavior as $r_{nm} \to \infty$. It is clear from Eq. (A6) that in general we must expect $\Phi_{nm}(r_{nm})$ to exhibit a relatively long ranged algebraic decay.

The physical significance of Eq. (A6) is readily understood. The first term is repulsive and falls as r^{-4}_{nm} as $r_{nm} \to \infty$. This contribution can be viewed as an attempt by the macroion to expel the neutral particle which is displacing polarizable material (i.e., solvent) from its environment. For a structureless continuum solvent [i.e., $h_{ns}(12) = 0$ if $r_{ns} > d_n/2$], $\Phi_{nm}(r_{nm})$ is totally determined by this repulsive interaction. Indeed, if we take ϵ to be given by the well-known Onsager formula then it is easy to verify that the term proportional to r^{-4}_{nm} is identical to the corresponding term in the classical cavity result.[17] Terms proportional to r^{-4}_{nm} and r^{-6}_{nm} have also been derived by Jepsen and Friedman[17] using cluster expansion methods.

The last two terms in Eq. (A6) depend upon the details of the correlation between the neutral particle and the solvent molecules. For the present model these terms make a net attractive contribution to $\Phi_{nm}(r_{nm})$ reflecting the fact that the neutral sphere is not easily accommodated by the water-like solvent. In effect, the macroion would like to repel the neutral particle but the molecular solvent pushes it back. The observed potential of mean force is the sum of these competing contributions.

[1] C. W. Outhwaite, in *Statistical Mechanics, Vol. 2. A Specialist Periodical Report* (The Chemical Society, London, 1973).
[2] J. P. Valleau and L. K. Cohen, J. Chem. Phys. **72**, 5935 (1980).
[3] S. L. Carnie, D. Y. C. Chan, D. J. Mitchell, and B. W. Ninham, J. Chem. Phys. **74**, 1472 (1981).
[4] M. Lozada-Cassou, R. Saavedra-Barrera, and D. Henderson, J. Chem. Phys. **77**, 5150 (1982).
[5] S. L. Carnie, Mol. Phys. **54**, 509 (1985).
[6] C. W. Outhwaite and L. B. Bhuyian, J. Chem. Soc. Faraday Trans. 2 **79**, 707 (1983).
[7] S. L. Carnie and G. M. Torrie, Adv. Chem. Phys. **56**, 141 (1984).
[8] L. Blum, in *Fluid Interfacial Phenomena*, edited by C. A. Croxton (Wiley, New York, 1986).
[9] J. M. Caillol, D. Levesque, J. J. Weis, P. G. Kusalik, and G. N. Patey, Mol. Phys. **62**, 461 (1987).
[10] P. Fries and G. N. Patey, J. Chem. Phys. **82**, 492 (1985).
[11] P. G. Kusalik and G. N. Patey, J. Chem. Phys. **88**, 7715 (1988).
[12] G. M. Torrie, P. G. Kusalik, and G. N. Patey, J. Chem. Phys. **88**, 7826 (1988).
[13] C. Y. Lee, A. J. McCammon, and P. J. Rossky, J. Chem. Phys. **80**, 4448 (1984).
[14] J. P. Valleau and A. A. Gardner, J. Chem. Phys. **86**, 4162 (1987).
[15] L. L. Lee and D. Levesque, Mol. Phys. **26**, 1351 (1973).
[16] P. G. Kusalik and G. N. Patey (to be published).
[17] D. W. Jepsen and H. L. Friedman, J. Chem. Phys. **38**, 846 (1963).
[18] M. Plischke and D. Henderson, J. Chem. Phys. **88**, 2712 (1988).